Measurement of the thermal-expansion coefficient of nickel from 300 to 1000 K and determination of the power-law constants near the Curie temperature*

T. G. Kollie†

Metals and Ceramics Division, Oak Ridge National Laboratory, Oak Ridge, Tennessee 37830

(Received 11 April 1977)

A fused-quartz dilatometer was used to measure the thermal-expansion coefficient α of nickel between 300 and 1000 K. Measurements on National Bureau of Standards certified copper and tungsten standards with the dilatometer established the uncertainty in the α measurements on nickel as $\pm 0.8\%$ ($\pm 0.10 \times 10^{-6}$ K^{-1}), except within ± 2 K of the Curie temperature T_C where the uncertainty was about $\pm 1.6\%$. Results of 38 investigations of the expansion of nickel reported in the literature were analyzed critically, resulting in a compilation of α of nickel from 0 to 1500 K. Theories of thermal expansion were employed to separate α into its paramagnetic α_p and magnetic α_m components. The calculated values of α_m near T_C were fitted to the power-law equation, $\alpha_m = A(t^{-a} - 1)a^{-1} + B$, that describes critical phenomena near the critical temperature [$t = (T - T_C)T_C^{-1}$]. It was demonstrated that the critical exponents above and below T_C, a and a', respectively, are the same as those derived from specific-heat measurements and that $a = a' = -0.093$ (± 0.010) in agreement with scaling laws of critical phenomena.

I. INTRODUCTION

The Curie temperature T_C of nickel is 628.5 K and the melting temperature of nickel is 1728 K. At T_C, a solid-state change occurs in the electron structure, and nickel transforms from the ferromagnetic to paramagnetic state. About 40 determinations of the thermal expansion of solid nickel have been reported[1] during the past 75 years, spanning the temperature interval 0–1685 K. A critical analysis of these results showed:

(a) The thermal-expansion coefficients α for nickel of the various investigations are in poor agreement in the temperature intervals of data overlap, especially near T_C and above about 850 K. Differences of 10–30% are not uncommon.

(b) The nickel specimens used were seldom characterized as to their purity, microstructure, or heat treatment prior to measurement. Certain impurities change the α of nickel near T_C as well as increase or decrease T_C.

(c) The accuracies of most techniques used to measure α were not established by either a detailed error analysis or measurements on a standard. Measurement errors, rather than specimen impurities, are probably the basis for the poor agreement among the reported α's.

The measurements of α of nickel reported here were performed on a well-characterized specimen using a technique whose accuracy was established by measurements on standards certified by the National Bureau of Standards (NBS). The measurements on nickel span the temperature interval 300–1000 K, with particular emphasis near T_C. By combining these data with selected low- and high-temperature data from the literature, values of α for nickel were compiled for temperatures between 0 and 1500 K. Using this compilation and theoretical expressions for the thermal expansion, the paramagnetic thermal-expansion coefficient α_p of nickel was calculated. In addition, the ferromagnetic contribution α_m to the thermal-expansion coefficient was calculated and tested for the expected power-law temperature dependence near T_C.

II. EXPERIMENTAL TECHNIQUE

A computer-operated fused-quartz differential dilatometer was used to measure the thermal expansion of nickel from 300 to 1000 K. A brief description of the specimen and technique follows; the interested reader is referred to Kollie *et al.*[2] for more details.

A. Specimen

The nickel stock from which the specimen was machined had a density of 8.9192×10^3 kg/m^3 and was at least 99.965% pure. Major impurities were carbon, cobalt, and iron. These accounted for 91% of the total impurities (Table I). The nickel specimen was a right-circular cylinder, 78 mm in length and 6.4 mm in diameter. After machining, the specimen was annealed in the dilatometer at 945 K for 17 h. The resulting microstructure, Fig. 1, is typical of pure polycrystalline nickel and some nickel alloys.

B. Dilatometer

Figure 2 is a cross section of the fused-quartz[3] differential dilatometer. To provide vertical sta-

TABLE I. Impurities in nickel specimen. The average of quantitative spectrochemical analyses of two samples from the nickel bar used to make the specimen is given. Other quantitative techniques were used for carbon and the gases hydrogen, nitrogen, and oxygen. Nickel stock was obtained from Materials Research Corp., Orangeburg, N. J.

Impurity	ppm (wt)	Impurity	ppm (wt)
Aluminum	< 0.5	Magnesium	< 0.2
Boron	0.1	Manganese	< 0.3
Calcium	4.0	Niobium	1.2
Carbon	155.0	Nitrogen	< 1.0
Cobalt	65.0	Oxygen	2.0
Chromium	1.0	Sodium	1.6
Copper	5.0	Sulfur	< 4.0
Hydrogen	< 1.0	Titanium	< 5.0
Iron	100.0	Vanadium	0.3
Lithium	0.1	Zinc	< 0.4

Total impurities < 347.7 ppm (wt).

FIG. 1. Photomicrograph at 100× of nickel-bar stock from which specimen was made, showing microstructure typical of nickel and some nickel alloys after annealing, polishing, and etching.

bility for the specimen and to reduce temperature gradients along its length, the nickel specimen was placed in a cylindrical copper holder. The holder, with the specimen in it, was placed on the platform of the quartz support tube. The support tube was attached to an Invar base plate, which served as the reference plane for length-change (δL) measurements of the dilatometer. The δL was the difference between the expansion of the support tube and the summed expansions of the specimen and push rod.

An automated micrometer[4] was used to measure δL. As illustrated in Fig. 2, the micrometer consisted of a motor-driven micrometer screw, whose contact with the push rod was sensed electrically. The micrometer provided three length-measurement signals. One signal was a mechanical counter; the other two signals were via an electronic counter, whose pulses were decoded and displayed at the micrometer control box and relayed to the computer-controlled data system. The uncertainty in α due to uncertainties in δL was determined by the micrometer linearity, which was shown by experiment to be $\pm 5 \times 10^{-6}$ cm.

C. Furnace and protection tube

A vertically mounted tube furnace was used to heat the dilatometer. To minimize temperature gradients in the specimen and its environs, the

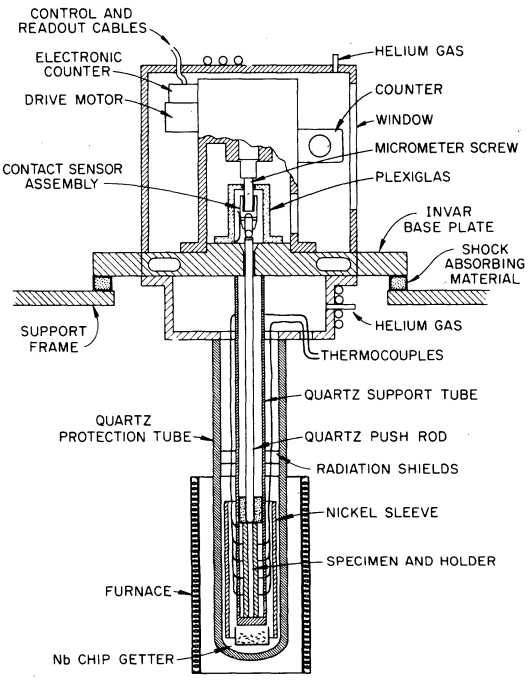

FIG. 2. Cross section of the fused-quartz differential dilatometer showing the major components of the apparatus.

specimen and lower portion of the support tube and push rod were put inside a nickel sleeve. Radiation shields were placed near the top of the furnace to reduce thermal radiation transfer to the base plate and to minimize the "chimney effect" of the helium gas in the protection tube.

A quartz protection tube was used to maintain a pure helium atmosphere around the lower portion of the dilatometer, thereby preventing oxidation of the metallic components and the specimen. Niobium chips, which have a high affinity for oxygen, were suspended below the specimen to further purify the atmosphere.

D. Temperature measurements

Temperatures of the specimen were measured using $Pt_{90}Rh_{10}$-vs-Pt thermocouples calibrated[5] on the International Practical Temperature Scale of 1968 (IPTS-68). Intrinsic measuring junctions of three thermocouples were spot welded to the specimen holder at equal spacings along its length. The outputs of the thermocouples were read by an analog-to-digital convertor,[2] which was interfaced with the computer-controlled data system. Uncertainties in temperature-change (ΔT) measurements were estimated[2] to be less than ± 0.27 K.

E. Computer data system

Operation of the dilatometer was completely automated using a minicomputer.[6] Tasks performed by the computer included: measuring the thermocouple emf's and converting these emf's to temperatures, reading the output of the micrometer, recording the specimen temperature and length measurements, and controlling the furnace temperature and the thermocycle of the experiment. Execution of these tasks was under control of programs written in a conversational, interpretative language called FOCAL. The interested reader is referred to articles by Kollie *et al.*[2,7] for details of the computer system.

F. Measurement procedure

The dilatometer was heated in succession to a preselected sequence of temperatures. Thermal equilibrium was established at each temperature of the sequence. This procedure allowed reproducible temperature profiles to be established in the dilatometer, which was necessary for accurate measurement of δL. When the furnace reached the first temperature of the sequence, the micrometer output was read six times and the specimen temperature read 50 times and the six lengths and average temperature were printed on the computer Teletype. The length and temperature measurements were repeated until the specimen temperature changed less than ± 0.01 K in 15 min. The temperature of the furnace was then changed to the next set point. After about a 2-h wait for thermal equilibrium, the specimen length and temperature measurements were begun.

G. Calculation procedure

A specimen of NBS-certified fused silica was used to calibrate the dilatometer from 300 to 1000 K. The calibration data, $L_C(T)$, and the certified expansion $\int \alpha_s dT$, were employed to calculate the length $L(T)$ of a test specimen at temperature T by

$$L(T) = L_0 + \delta L(T) - \delta L(T_0) + L_0 \int_{T_0}^{T} \alpha_s dT - L_C(T), \tag{1}$$

where L_0 was the length of the specimen at $T_0 = 295$ K, and $\delta L(T)$ and $\delta L(T_0)$ were the micrometer readings at T and T_0, respectively.

The thermal-expansion coefficient α of the test specimen was calculated by either of two methods. When the temperatures T_2 and T_1 of two data points differed by more than about 20 K, a point-to-point method was employed using the equation

$$\alpha = \frac{1}{L_0}\frac{\Delta L}{\Delta T} = \frac{1}{L_0}\frac{L(T_2) - L(T_1)}{T_2 - T_1}, \tag{2}$$

and the α was assigned to the average temperature $0.5(T_2 + T_1)$. The second method consisted of least-squares-fitting several $L(T)$ data points to a polynomial $f(T)$, and α was computed by differentiating the polynomial with respect to T and dividing by L_0, that is,

$$\alpha = \frac{1}{L_0}\frac{df(T)}{dT}. \tag{3}$$

This second method was used when the temperatures of the data points were close together as, for example, for measurements near T_C of nickel. The α calculated from Eq. (3) was assigned to the mean temperature of the data used in the fit.

H. Measurements on standards

To establish the accuracy of the dilatometer, the α of NBS-certified copper was determined from 300 to 800 K, the upper temperature of the certification, and the α of NBS-certified tungsten was determined from 300 to 1000 K. The measurements on tungsten ($\alpha \simeq 5\times10^{-6}$ K^{-1}) provided the more severe test of the accuracy of the dilatometer, but the measurements on copper ($\alpha \simeq 18 \times 10^{-6}$ K^{-1}) approximately spanned the α range of nickel ($\alpha \simeq 16\times10^{-6}$ K^{-1}).

Figure 3(a) shows the difference between the

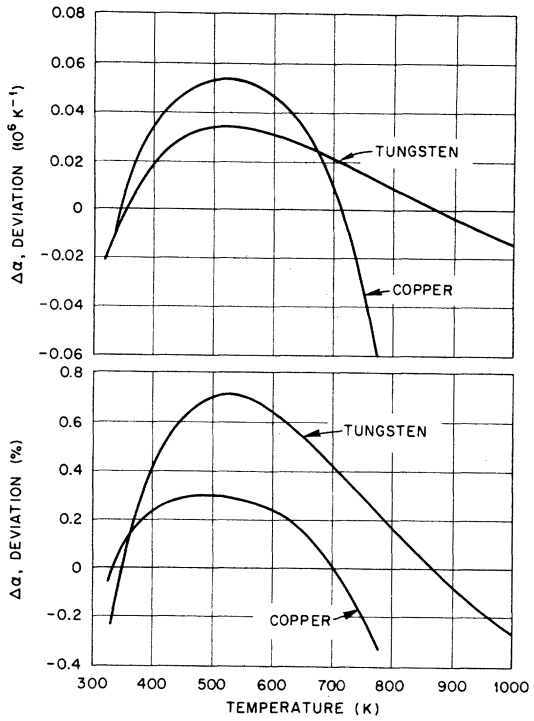

FIG. 3. Deviation $\Delta\alpha$ between α measured with dilatometer and α of NBS-certified copper and tungsten specimens: (a) $\Delta\alpha$ plotted in K^{-1} vs temperature, showing that $\Delta\alpha$ was less than $\pm 0.06\times10^{-6}$ K^{-1} on both specimens; (b) $\Delta\alpha$ plotted in percent vs temperature, showing maximum deviations of $\pm 0.3\%$ on copper and $\pm 0.7\%$ on tungsten.

measured and NBS-certified values of α for copper and tungsten, and Fig. 3(b) is the same data plotted on a percentage basis.[8] The measured α's for copper and tungsten were within ±0.3 and ±0.7%, respectively, of the NBS certification. Because NBS estimated their measurement uncertainties as about ±0.2% for copper and ±1.0% for tungsten, the maximum uncertainties in the dilatometer were established by these experiments to be ±0.5% ($\pm0.10\times10^{-6}$ K^{-1}) for copper and ±1.7% ($\pm0.08\times10^{-6}$ K^{-1}) for tungsten. Based on the measurements on the copper standard, an uncertainty of $\pm0.10\times10^{-6}$ K^{-1} (±0.8%) is claimed for the measurements on nickel, except near T_C. Within about ±2 K of T_C, the uncertainties may be doubled to ±1.6% because the calculation procedure using Eq. (3) caused rounding of the maximum in α at T_C, as discussed below.

III. RESULTS

A total of 291 data points, each consisting of a length and a temperature measurement, were obtained on the nickel specimen between 300 and 1000 K. These data points were divided into six overlapping temperature intervals in which the α of nickel was calculated as a function of temperature using Eqs. (2) or (3). The calculated α-T points of each interval were plotted on graph paper, and a smooth curve was passed through the points so that their deviations from the curve were minimized and so that a smooth and continuous curve was obtained with adjacent intervals.[9] The standard deviation σ of the 348 calculated α-T points about the smooth curve was $\pm0.056\times10^{-6}$ K^{-1}. Thus, the claimed uncertainty in the measurements on nickel, $\pm0.10\times10^{-6}$ K^{-1}, is at the 93% confidence level for a normal distribution of deviations. Table II is a list of the smooth values of α of nickel.

As shown in Fig. 4, the α of nickel goes through a sharp maximum near T_C. To determine the true α-vs-T relationship near T_C, data points had to be taken with small ΔT's between them. If Eq. (2) was used to calculate α, the uncertainty in α increased as ΔT decreased. Use of the least-squares-fitting procedure and Eq. (3) reduced these uncertainties, except close to T_C, where this procedure rounded the maximum in α. The amount of rounding depended on the temperature span of the data used in the fit and the ΔT between the data points. For example, in the interval 610–645 K, third-order polynomials in T were fitted through sets of 11 data points, at ΔT's of 1 K, that spanned 10 K. The rounding that resulted within ±2 K of T_C is evident in data sets A and B of Fig. 5.

Attempts to improve the resolution in α near T_C, using data points at ΔT's less than 1 K, were hindered by a $\pm5\times10^{-6}$-cm nonlinearity in the micrometer. It was possible, however, to calibrate out the nonlinearity by measurements of δL of a copper specimen with small ΔT's between data points. After calibration, nine data points taken with ΔT's of 0.4 K and spanning about 4 K were fitted to third-order polynomials in T. This procedure and Eq. (3) was used to calculate α in the temperature interval 625–631 K, resulting in the α-T points represented by set C in Fig. 5. The rounding of the maximum in α was confined to temperatures between 628.2 and 628.6 K.

The principal concern during measurements between 713 and 1000 K was creep of the specimen, but data taken on heating to and cooling from 1000 K were in excellent agreement, which would not have been the case had creep occurred. In fact, the σ ($\pm0.04\times10^{-6}$ K^{-1}) of the α-T points calculated between 713 and 1000 K was the smallest of the data in the six temperature intervals.

IV. COMPARISON OF RESULTS

As discussed in the Introduction, differences of 10–30% are not uncommon among the 38 previous

determinations[1] of the thermal expansion of nickel. The differences $\Delta\alpha$ between the α's of 34 investigations reporting data from 300 to 1000 K and those of this investigation were calculated. Of these, the $\Delta\alpha$'s of 26 investigations were greater than ±5%, especially near T_C and above 800 K; most notable was the oft-quoted work of Nix and MacNair.[10] A brief comparison of the results of the eight other investigations[11–18] is as follows.

Near T_C, only the measurements of Major *et al.*[12] are reported in sufficient detail for comparison, and these data are plotted in Fig. 5 with the values of α obtained in this investigation. Below T_C, the results of Major *et al.* are essentially parallel to and 1% below the α of this investigation. Above T_C, the temperature dependences of α of Major *et al.* differ significantly from those of the author, especially between T_C and T_C+4 K (628.5–632.5 K). Although not shown in Fig. 5, the α's reported by Major *et al.* above T_C continue to decrease mono-

TABLE II. Thermal-expansion coefficients of nickel.[a]

T (K)	Thermal-expansion coefficients α (10^6 K^{-1})	α_t (10^6 K^{-1})	α_m (10^6 K^{-1})	T (K)	Thermal-expansion coefficients α (10^6 K^{-1})	α_t (10^6 K^{-1})	α_m (10^6 K^{-1})
10	0.05[b]	0.05	0.00[e]	613	17.32	17.24	2.00
20	0.16[b]	0.16	0.00	614	17.36	17.28	2.03
40	1.10[c]	1.10	0.00	615	17.40	17.32	2.06
60	2.80[c]	2.80	0.00	616	17.45	17.37	2.11
80	4.72[c]	4.73	0.00	617	17.49	17.41	2.14
100	6.46[c]	6.47	0.00	618	17.54	17.46	2.18
140	8.96[c]	8.98	0.00	619	17.59	17.51	2.22
180	10.50[c]	10.52	0.00	620	17.66	17.57	2.28
220	11.52[c]	11.53	0.00	621	17.72	17.63	2.33
260	12.25[c]	12.26	0.07	622	17.78	17.69	2.38
300	12.89	12.89	0.20[e]	623	17.86	17.77	2.45
400	14.17	14.15	0.51	624	17.95	17.86	2.54
500	15.35	15.31	0.89	625	18.04	17.95	2.62
520	15.63	15.58	1.01	626	18.16	18.07	2.73
540	15.92	15.86	1.15	627	18.37	18.28	2.94
560	16.24	16.18	1.32	628	18.79	18.70	3.35
580	16.57	16.50	1.50	628.2	18.95	18.86	3.50
600	16.96	16.88	1.73	629	18.09	18.00	2.64
605	17.08	17.00	1.81	630	17.71	17.62	2.25
610	17.22	17.14	1.92	631	17.48	17.39	2.02
611	17.25	17.17	1.94	632	17.31	17.22	1.84
612	17.28	17.20	1.96	633	17.20	17.11	1.72
634	17.12	17.03	1.63	650	16.53	16.44	0.93
635	17.06	16.97	1.57	668	16.47	16.37	0.73
636	17.00	16.91	1.50	688	16.48	16.37	0.58
637	16.94	16.85	1.43	708	16.50	16.38	0.45
638	16.90	16.81	1.39	763	16.64	16.49	0.15
639	16.86	16.77	1.34	863	17.36	17.15	0.05
640	16.82	16.73	1.29	973	18.27	17.98	0.00
641	16.79	16.70	1.25	1073	19.15[d]	18.81	0.00
642	16.75	16.66	1.21	1173	20.10[d]	19.71	0.00
643	16.72	16.63	1.17	1273	21.07[d]	20.61	0.00
644	16.68	16.59	1.12	1373	22.11[d]	21.58	0.00
645	16.65	16.56	1.08	1473	23.19[f]	22.59	0.00

[a] Thermal-expansion coefficients: α, coefficient relative to room-temperature length; α_t, coefficient relative to length at temperature and is the thermodynamic coefficient and equals $\alpha_m+\alpha_p$; α_p, coefficient of paramagnetic nickel; α_m coefficient of ferromagnetic component of α_t.

[b] Data from White (Ref. 31).

[c] Data from Clark (Ref. 32).

[d] Data from Totskii (Ref. 15) corrected up 0.13×10^{-6} K^{-1}.

[e] Values of α_m may be in error between 10 and 300 K because the high-temperature Debye temperature (Ref. 19) of nickel, 385 K, was used to calculate α_p, as discussed in the text.

[f] Extrapolated using Eq. (8) with $C=12.23\times10^{-6}$ K^{-1}, $D=4.144\times10^{-9}$ K^{-2}, and $E=5.714\times10^{-12}$ K^{-3}.

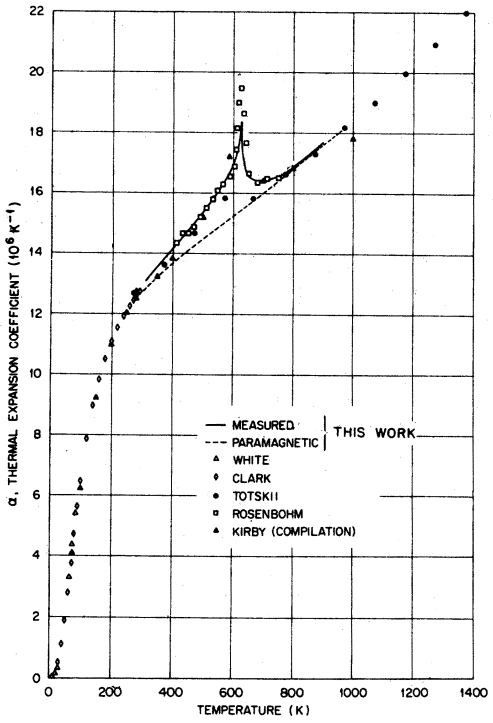

FIG. 4. The α of nickel vs temperature of this work and those of White (Ref. 31), Clark (Ref. 32), Totskii (Ref. 15), Rosenbohm (Ref. 13), and the compilation of Kirby (Ref. 11), and the calculated paramagnetic thermal-expansion coefficient of nickel.

tonically to 690 K, the upper temperature limit of their measurements; the author's measurements, however, show that α begins to increase above 653 K. At 690 K, the difference between these two sets of measurement of α is 6%, which is three times larger than the combined uncertainties (±1.8%) of the two techniques.

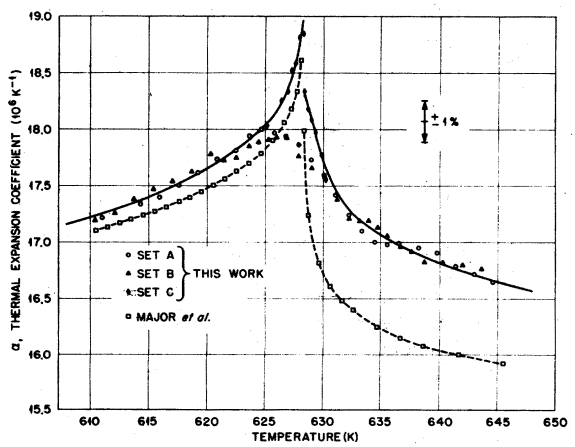

FIG. 5. The α of nickel vs temperature near the Curie transformation temperature (628.5 K), showing results of this work (sets A–C; see text for explanation) and that of Major *et al*. (Ref. 12).

The best agreement with the author's measurements are the α's calculated from $\Delta L/L_0$ vs T reported by Rosenbohm[13] for temperatures between 400 and 750K. In particular, Rosenbohm's measurements and those of the author have approximately the same temperature dependence and differ by less than ±1.5%. Jordan and Swanger's[14] reported α's are also within ±1.5% of the author's between 350 and 650 K, but deviate negatively between 800 and 1000 K, possibly owing to errors caused by creep of their specimen at these elevated temperatures.

Totskii[15] reported eight values of α between 300 and 1000 K. Two of these points, at 573 and 673 K, were calculated using length measurements that spanned T_C and $\Delta\alpha$ is approximately-4% for both these points. Totskii's α-T points at 773, 873, and 973 K are less than 1% below those of this investigation and show approximately the same temperature dependence. For this reason, Totskii's measurements above 1000 K were used in the compilation of Table II.

The $\Delta\alpha$'s calculated from the measurements of Pathak *et al.*[16] are about 5% high at 573 and 773 K but are less than 1% low below 523 K. Arbuzov and Zelekow's[17] reported values of α oscillate about those of the author but show approximately the same temperature dependence above 800 K. Between 300 and 1000 K, the compilations of Kirby[11] and Touloukian *et al.*[18] appear to be weighted heavily by the measurements of Jordan and Swanger.[14]

V. ANALYSIS OF RESULTS

A. Background

The thermal-expansion coefficient α is a thermodynamic quantity defined by

$$\alpha = \frac{1}{3V}\left(\frac{\partial V}{\partial T}\right)_P = \frac{1}{3V}\left(\frac{\partial}{\partial T}\left[\frac{\partial G}{\partial P}\right]_T\right)_P = \frac{1}{3V}\left(\frac{\partial^2 G}{\partial T \partial P}\right)_{PT}, \quad (4)$$

where V is the specific volume, P the pressure, and G the specific Gibbs free energy. At the Curie temperature T_C, the ferromagnetic phase of nickel transforms to the paramagnetic phase. Because a volume change does not occur in nickel at T_C, the first-order derivates of G are continuous. The shape of the α-vs-T curve at T_C, Figs. 4 and 5, suggests that α may have a singularity at T_C and, thus, the second-order and higher derivatives of G could be discontinuous. However, it is experimentally difficult, if not impossible, to determine

unequivocally if α of nickel is discontinuous at T_C. The same is true for measurements at T_C of other thermodynamic quantities of nickel, such as the specific heat[19-23] at constant pressure C_P. Part of the experimental difficulty arises because determinations of α and C_P require differentiation of one measured quantity with respect to another—for α, dL/dT, and C_P, dT/dZ, where Z is the time. Another problem is that specimen imperfections, such as impurities and possibly dislocations, cause small variations in T_C throughout the specimen, resulting in a "rounding" of α and C_P near T_C.

In spite of these experimental difficulties, treatment of the Curie transformation as a second-order discontinuity in the derivatives of G has been of considerable theoretical interest because the Curie transformation is one of a broad class of transformations called "critical phenomena." Much of the interest in critical phenomena has been directed at the study of the critical exponents of the power-law equations which describe the singularities in the thermodynamic quantities near T_C. Also, the scaling hypothesis,[24] which states that G is a homogeneous function of the reduced temperature $t=(T-T_C)T_C^{-1}$, yields relationships between the critical exponents for $T>T_C$ and $T<T_C$ and between the critical exponents of various thermodynamic quantities. The power-law equations for α are

$$\alpha=(A'/a')(t^{-a'}-1)+B' \quad (T<T_C), \tag{5}$$

$$\alpha=(A/a)(t^{-a}-1)+B \quad (T>T_C), \tag{6}$$

where the constants a' and a are the critical exponents and A, A', B, and B' are constants. Just as was shown[24-26] for C_P measurements, it was also difficult to determine unique and unambiguous values for the constants of Eqs. (5) and (6) from α measurements near T_C. The values determined for the constants depend on: the analytical method used to fit the experimental values of α to the power laws; the temperature interval of the α data used in the fit; the number of data points in the interval; the distribution of the data points in the interval; and the method used to subtract out the nonsingular, but temperature-dependent, components of α. Also, the rounding of α near T_C makes the choice of the value of T_C used to calculate t somewhat subjective. For example, Major *et al.*[12] chose T_C to be 0.1 K above the temperature of the maximum in α. The procedure used by this author in the obtaining of the power-law constants is outlined below.

B. Procedure

The α's calculated using Eqs. (2) and (3) are referred to the room-temperature specimen length L_0, whereas the thermodynamic definition of α given in Eq. (4) is referred to the length $L(T)$ $[V=3L(T)]$. The thermodynamic expansion coefficient α_t, listed in Table II, was calculated by multiplying the α's obtained from Eqs. (2) and (3) by the ratio $L_0/L(T)=(1+\int_{T_0}^{T}\alpha dT)^{-1}$. To subtract out the nonsingular component of α_t, the paramagnetic thermal-expansion coefficient α_P was calculated from Grüneisen's approximation[27] with the assumption that the product of the Grüneisen constant γ and the specific heat at constant volume C_v were separable into electronic, $\gamma_e C_{ve}$, harmonic, $\gamma_h C_{vh}$, and anharmonic, $\gamma_a C_{va}$, components[28]:

$$\alpha_p=\frac{K}{3V_p}(\gamma C_v)=\frac{K}{3V_p}(\gamma_e C_{ve}+\gamma_h C_{vh}+\gamma_a C_{va}). \tag{7}$$

For paramagnetic nickel, K is the isothermal compressibility and V_P is the specific volume. After substituting the temperature-dependent expressions[23,28] for C_{ve}, C_{vh}, and C_{va} into Eq. (7), it was assumed that K/V_p was constant, yielding

$$\begin{aligned}\alpha_p&=(K/3V_p)[\gamma_e A_e T+\gamma_h f(\Theta/T)+\gamma_a(A_a T+B_a T^2)]\\&=CT+DT^2+Ef(\Theta/T),\end{aligned} \tag{8}$$

where A_e, A_a, B_a, C, D, and E are constants and $f(\Theta/T)$ is the Debye function with Debye temperature Θ.

At high temperature, α_t is essentially equal to α_p; that is, the ferromagnetic component α_m, which causes the singularity in α_t at T_C, is approximately zero above about 1000 K ($\alpha_t=\alpha_p+\alpha_m$). The α_t data between 973 and 1373 K (Table II) were fitted to Eq. (8) by the method of least-squares to determine C, D, and E; in this temperature interval, $f(\Theta/T)$ is constant. Values of α_p between 240 and 973 K were calculated using Eq. (8) with a high-temperature Debye temperature[29] of 385 K and are plotted in Fig. 4. Values for α_m were calculated by subtracting α_p from α_t.

The power-law constants were obtained by fitting α_m to Eqs. (5) and (6) using the method of least squares. The temperature intervals to be used in the fits were determined by plotting $\log(d\alpha_m/dT)$ versus $\log(|T-T_C|)$, which was a straight line in the temperature intervals in which α_m was described by Eqs. (5) and (6). For $T<T_C$ the interval was 608–627.6 K, and for $T>T_C$ the interval was 629–645 K. Data points at about 1-K intervals were used in the fit.

Because the experimentally determined temperature of the maximum in α could be shifted between 628.2 and 628.6 K by varying the calculation procedure, as discussed, an uncertainty of 0.4 K existed in T_C. Thus, values of the power-law constants were computed for several T_C's, as listed in Table III. When T_C was set at 628.2 K,

TABLE III. Values of the constants of the power-law equations obtained from least-squares fits of α_m.

T_C (K)	a' (±0.01)	a (±0.01)	A' (10^6 K^{-1})	A (10^6 K^{-1})	A/A'	B' (10^6 K^{-1})	B (10^6 K^{-1})	σ' (10^6 K^{-1})	σ (10^6 K^{-1})
628.53[a]	−0.093	−0.093	0.639[e]	0.736[f]	1.15[g]	0.00(±0.07)	−1.18(±0.08)	±0.009	±0.012
628.2[b]	−0.18	+0.02	0.899[e]	0.452[f]	0.50[g]	−0.44(±0.03)	−0.61(±0.24)	±0.007	±0.034
628.3[c]	−0.14	−0.01	0.758[e]	0.524[f]	0.69[g]	−0.20(±0.04)	−0.76(±0.96)	±0.008	±0.033
628.0[d]	−0.22	•••	1.038[e]	•••	•••	−0.64(±0.02)	•••	±0.006	•••
628.4[d]	•••	−0.04	•••	0.589[f]	•••	•••	−0.89(±0.17)	•••	±0.011

[a] See Fig. 6.
[b] Temperature of maximum in α.
[c] Temperature of maximum in $\alpha + 0.1$ K.
[d] Determined from least-squares fit.
[e] σ of $\pm 0.004 \times 10^{-6}$ K^{-1}.
[f] σ of $\pm 0.005 \times 10^{-6}$ K^{-1}.
[g] σ of ±0.02.

the temperature of the maximum of α in Figs. 4 and 5, a' equaled -0.18 and a equaled +0.02. Increasing T_C by 0.1 K to 628.3 K raised a' to -0.14 and lowered a to -0.01. If T_C was also obtained from the fit, a' equaled -0.22 at a T_C of 628.0 K and a equaled +0.04 at a T_C of 628.4 K.

The scaling laws state that $a' = a$. To determine T_C for $a' = a$, least-squares values of a' and a were obtained as a function of T_C and are plotted in Fig. 6. The curves of a' vs T_C and a vs T_C intersect at $a' = a = -0.093$ and $T_C = 628.53$ K.

C. Comparison of analysis

Major *et al.*[12] obtained $a' = -0.27$ (±0.05) and $a = 0.05$ (±0.05) for T_C raised 0.1 K above the temperature of the maximum in α. For the equivalent T_C, the data of Table III show $a' = -0.14$ (±0.01) and $a = -0.01$ (±0.01). This poor agreement with the critical exponents of Major *et al.* is attributed to their fitting α to the power laws for temperatures outside the critical region ($|T - T_C|$ as large as 63 K), to their not subtracting α_p from α before fitting to the power laws, and to errors in their measurements at $T > T_C$.

A scaling relationship introduced by Buckingham and Fairbank[30] suggests that the singularities at T_C of C_P and α should have the same critical exponents. Lederman *et al.*[26] and Cook[25] determined that the C_P measurements on nickel of Connelly *et al.*[19] showed the best agreement with the power and scaling laws near T_C. Connelly *et al.* fitted their C_P data to the power laws and found $a' = -0.18$ (±0.03) and $a = 0.00$ (±0.03) when T_C was set equal to the temperature of the maximum in C_P. For the equivalent T_C, the data of Table III show $a' = -0.18$ (±0.01) and $a = +0.02$ (±0.01). When Connelly *et al.* determined $a' = a$ as in Fig. 6, they obtained $a' = a = -0.10$ (±0.03) for a T_C 0.13 K above the temperature of the maximum in C_P. From Fig. 6, the author obtained $a' = a = -0.093$ (±0.010) for a T_C 0.33 K above the temperature of the maximum in α. These comparisons demonstrate that α and C_P do indeed have the same critical exponents near T_C.

The scaling laws for C_p predict $a' = a = -0.10$, which is in excellent agreement with the C_p measurements of Connelly *et al.* and the α measurements of this author. In addition, Lederman *et al.*[26] showed that for Heisenberg ferromagnets, such as nickel, the amplitude ratios $A/A' = 1.11$ (±0.09) when $a' = a = -0.10$ (±0.01). The value of A/A' of Connelly *et al.* is 1.14 (±0.04) and, from Table III, the author's value is $A/A' = 1.15$ (±0.02), both for $a' = a \approx -0.10$.

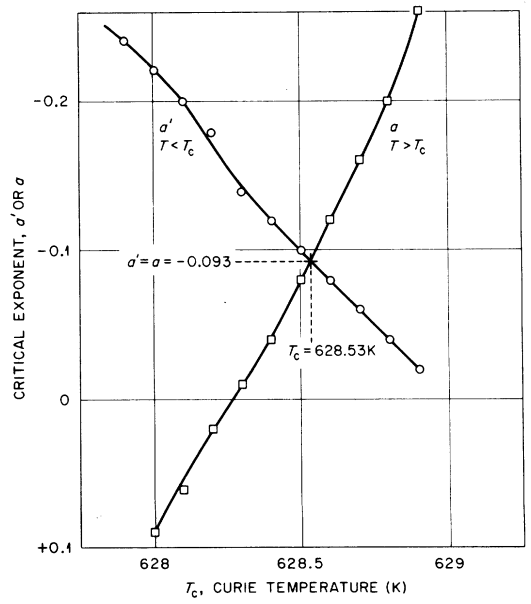

FIG. 6. Critical exponents a' and a as function of the temperature selected for the Curie temperature T_C, showing that fits of data to power law above T_C and below T_C intersect at $a' = a = -0.093$ and $T_C = 628.53$ K.

D. Critique of the analysis

In summary, least-squares fits of α_m to the power laws demonstrated that the thermal-expansion coefficient and the specific heat of nickel have the same critical exponents and ratio of A/A' and that both of these thermodynamic quantities obey the scaling laws $a' = a = -0.10$. One criticism of the least-squares method is that the standard deviations σ of the fits, which are measures of the qualities of the fit, showed little dependence on T_C, but small changes in T_C caused large changes in the constants of the power-law equations (Table III). In addition, the σ's are about an order of magnitude smaller than the uncertainty ($\pm 0.10 \times 10^{-6}$ K^{-1}) in the measurements of α, and some σ's are even smaller than the resolution of measurement of α (about 0.01×10^{-6} K^{-1}). Consequently, the value of T_C, which is difficult to measure experimentally because of rounding of α and C_p near T_C and which may not equal the temperature of the maximum in α or C_p, cannot be determined directly from least-squares fits. As shown in Table III, least-squares values of T_C obtained from fits of α_m above and below T_C differ by 0.4 K, and the critical exponents that resulted from these two fits did not obey the scaling law $a' = a = -0.10$.

Use of the plot shown in Fig. 6 to force a' to equal a may seem artificial. However, Cook[25] used an analytical fitting procedure that was much more sophisticated than the method of least squares and derived $a' = -0.09$ (± 0.03), $a = -0.14$ (± 0.02), and $A/A' = 1.39$ (± 0.22) from the C_p measurements of Connelly *et al.*[19] Thus, the results of the analysis shown in Fig. 6, which was also used by Connelly *et al.* to obtain $a' = a = -0.10$ from their C_p measurements, appears justified.

ACKNOWLEDGMENTS

The author is pleased to acknowledge Dr. D. L. McElroy and Dr. R. L. Anderson for their helpful suggestions and review of the manuscript. F. C. Weaver and T. G. Godfrey are thanked for their efforts in the data analysis.

---

*Research sponsored by the U. S. Energy Research and Development Administration under contract with the Union Carbide Corp.

†Present address: Oak Ridge Y-12 Plant, Oak Ridge, Tenn. 37830.

[1]A literature survey and data retrieval of measurements of the thermal expansion of nickel were performed for the author by CINDAS, located at Purdue University in West Lafayette, Ind.

[2]T. G. Kollie, D. L. McElroy, J. T. Hutton, and W. M. Ewing, AIP Conf. Proc. 17, 129 (1974).

[3]The term quartz is used synonymously with *fused quartz*.

[4]Carson-Dice Electronic Micrometer model 71-A-9 and Decoder and Controller model DR-B-4.

[5]A comparison calibration, with uncertainties of ± 0.2 K, was performed using $Pt_{90}RH_{10}$-vs-Pt standard thermocouples calibrated by the NBS.

[6]Digital Equipment Corp. PDP-8 computer.

[7]T. G. Kollie, D. L. McElroy, R. K. Adams, and J. M. Jansen, in *Temperature—Its Measurement and Control in Science and Industry* (Instrument Society of America, Pittsburgh, 1972), Vol. 4, p. 1457.

[8]The deviations shown in Fig. 3 for copper differ from Fig. 8 of Kollie *et al.* (Ref. 2) because the original NBS certification for copper was in error (−2% max) between 600 and 800 K. These errors were caused by creep of the NBS copper specimen during measurements above 600 K and were eliminated by modification of the NBS technique. Similarly, the deviations for tungsten shown in Fig. 3 differ from Fig. 9 of Kollie *et al.* because of a temperature-measurement error (0.5 K) in the dilatometer between 900 and 1000 K. These errors were due to leakage currents on the thermocouples caused by thermionic emission between the nickel sleeve and copper specimen holder (Fig. 2) and were eliminated by grounding the sleeve and holder.

[9]This procedure was preferred because least-squares fitting, for example, would force the α of nickel to assume a functional temperature dependence that would bias the theoretical analysis of the data.

[10]F. C. Nix and D. MacNair, Phys. Rev. 60, 597 (1941).

[11]R. K. Kirby, in *American Institute of Physics Handbook*, 2nd ed. (McGraw-Hill, New York, 1963), pp. 4–64.

[12]J. Major, F. Mezei, E. Nagy, E. Svåb, and G. Ticky, Phys. Lett. A 35, 377 (1971).

[13]E. Rosenbohm, Physica 5, 385 (1938).

[14]L. Jordan and W. H. Swanger, J. Res. Natl. Bur. Stand. 5, 1291 (1930).

[15]E. E. Totskii, Teplofiz. Vys. Temp. 2, 205 (1964) [High Temp. (USSR) 2, 181 (1964)].

[16]P. D. Pathak, M. C. Gupta, and J. M. Trivedi, Ind. J. Phys. 43, 104 (1969).

[17]M. P. Arbuzov and I. A. Zelenkov, Fiz. Met. Metalloved. 18, 311 (1964).

[18]Y. S. Touloukian, R. K. Kirby, R. E. Taylor, and P. D. Desai, in *Thermophysical Properties of Matter* (Plenum, New York, 1975), Vol. 12, pp. 225–235.

[19]D. L. Connelly, J. S. Loomis, and D. E. Mapother, Phys. Rev. B 3, 924 (1971).

[20]W. E. Maher and W. D. McCormick, Phys. Rev. 183, 573 (1969).

[21]P. Handler, D. E. Mapother, and M. Rayl, Phys. Rev. Lett. 19, 356 (1967).

[22]Y. A. Kraftmakher, Fiz. Tverd. Tela 8, 1306 (1966) [Sov. Phys. Solid State 8, 1048 (1966)].

[23]T. G. Kollie, Ph.D. dissertation, University of Tennessee, 1969 (unpublished) (Oak Ridge National Laboratory Technical Memo ORNL-TM-2649).

[24]L. P. Kadanoff *et al.* Rev. Mod. Phys. 39, 395 (1967).

[25]F. J. Cook, J. Phys. Chem. Ref. Data 2, 11 (1973).
[26]F. L. Lederman, M. B. Salamon, and L. W. Shacklette, Phys. Rev. B 9, 2981 (1974).
[27]E. Grüneisen, in *Handbuch der Physik*, edited by F. Henning (Springer, Berlin, 1926), Vol. 10, p. 1.
[28]B. Yates, Thermal Expansion (Plenum, New York, 1972).
[29]R. J. Birgeneau *et al.*, Phys. Rev. 136, A1359 (1964).
[30]M. J. Buckingham and W. M. Fairbank, in *Progress in Low Temperature Physics*, edited by C. J. Gorter (North-Holland, Amsterdam, 1961), Vol. II, p. 80.
[31]G. K. White, Proc. Phys. Soc. London 86, 159 (1965).
[32]A. F. Clark, Cryogenics 8, 231 (1968).

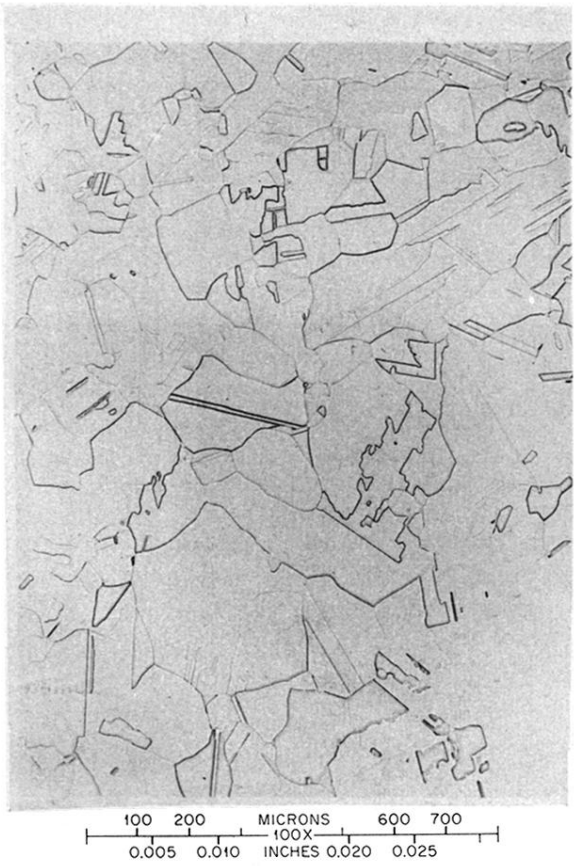

FIG. 1. Photomicrograph at 100× of nickel-bar stock from which specimen was made, showing microstructure typical of nickel and some nickel alloys after annealing, polishing, and etching.